

# A NEW CONTROL ALGORITHM OF SHUNT ACTIVE POWER FILTER UNDER DISTORTED GRID VOLTAGE AND UNBALANCED SUPPLY CONDITIONS

K. Shabana Banu<sup>1</sup>, R. Jaya shubha <sup>2</sup>

<sup>1</sup> PG scholar, Department of EEE, JNTU Anantapur, Andhra Pradesh, India

<sup>2</sup> PG scholar, Department of EEE, JNTU Anantapur, Andhra Pradesh, India

**Abstract:** To achieve maximum possible power factor and by keeping total harmonic distortion (THD) within the acceptable limit. A new control algorithm of shunt active power filter under distorted grid voltage and unbalanced supply conditions is proposed. A new control algorithm renders the optimal compromise between harmonic free (HF) and unity power factor (UPF) by keeping the total harmonic distortion (THD) of the source current within the standard range. In this paper, a new control approach for a three-phase four-wire shunt active power filter with PI and FUZZY controller under distorted grid voltage and unbalanced supply conditions is proposed. The algorithm employs a one-step process to get the conductance factors (only three). The extracted balanced set of voltages is multiplied with the constant conductance factors to get the required source currents. Using lagrangian technique mathematical formulas are derived for the conductance factors. Synchronous reference frame (SRF) theory is used to extract a balanced set of voltages from asymmetrical and distorted supply voltage conditions. Results acquired by simulations with Matlab/Simulink shows that the proposed control algorithm is very flexible and effective under steady and dynamic load conditions when compared to iterative OCA.

**Key Terms-** Shunt Active power filter (SAPF), unity power factor (UPF), total harmonic distortion (THD), PI controller, fuzzy controller.

## 1 .INTRODUCTION

Now a days, Increase of nonlinear loads in electrical power systems drives the unbalanced currents which results in power distortion. Excessive neutral currents, poor power factor, unbalanced voltage, increased losses, reduction in overall efficiency take place in the system with the increase of load current unbalance. To get control of such power quality problems shunt Active power filters (APFs)

are mostly used. Based on estimated reference currents, harmonic and reactive compensation currents are injected to regulate the shunt APF. These inculcated reference currents are meant to nullify the harmonic and reactive currents drawn by the nonlinear loads. Recently, fuzzy logic controller is introduced in numerous power electronics applications and has created a great deal of Interest.

To get the required compensation characteristics for SAPF, selection of control strategy plays a dominant role. Perfect harmonic cancellation strategy (HF) and unity power factor (UPF) strategy are the two major control strategies for load compensation [3]-[13]. Distortion-free source currents are produced by the HF strategy, whereas for a given average load power UPF control strategy produces minimum RMS values of source current [4]. The prime advantage of UPF is that the damping produced by the compensated resistive part of the load can be preserved. In case of resonance phenomena this damping effect is required, especially in the voltage distorted grids, in case of failing high voltage distortion is produced at the point of common coupling (PCC).

There are two main categories for the shunt APF based on optimization control strategy under distorted grid voltages and unbalanced supply conditions. In the first category, the distorted grid and unbalanced supply voltages of each phase are elapsed over a set of filters, such as band pass. To get the required compensated voltages, these filter gains are optimized by considering voltage total harmonic distortion (THD) and voltage UB limit as constraints. To obtain the required source currents the compensated voltages are multiplied with constant conductance factors. In the second category, optimization problem is formulated by taking conductance factors as variables to minimize the complexity and dimensionality of the optimization problem. For each harmonic order the conductance factors are optimally determined. Then a

balanced set of supply voltages are multiplied with these conductance factors to get the required source currents.

To solve the optimization problem in the aforementioned optimization algorithms iterative techniques has used. Hence iterative technique can result in a computational delay. Thus these iterative control approaches focused on steady state load conditions and inhibits dynamic load compensation.

To conquer above mentioned challenges, a new control algorithm for a three-phase four-wire shunt active power filter with PI and FUZZY controller under distorted grid voltage and unbalanced supply conditions is proposed. A new control algorithm does not use any iterative optimization technique. It calculates conductance factors directly without using any iterative optimization technique. To achieve the required performance no need to evaluate the conductance factors for every harmonic order separately, three conductance factors (one for the basic harmonic and other two alternatives for odd and even harmonics) are sufficient. The proposed algorithm can effectively work under steady-state as well as dynamic load conditions due to direct calculation of the conductance factors (only three) without using any iterative technique. A new control algorithm is developed by lagrangian formulation. Further, synchronous reference frame (SRF) theory is used to extract a balanced set of voltages from distorted grid and unbalanced supply voltages.

The advantage of fuzzy logic controller is that they do not need an precise mathematical model upon the accustomed PI controller. When compared to conventional PI controller, Fuzzy controller is more robust, can handle nonlinearity and works with indistinct inputs. For harmonics mitigation and power quality improvement Fuzzy logic controller is used under variable load conditions. This paper, therefore, presents an improved performance of shunt active power filter using Mamdani fuzzy-controller to control the harmonics under distorted grid voltages and unbalanced supply conditions.

### 1.1 The 4-Leg Shunt Active Power Filter

The Four-leg VSI-based shunt APF system configuration is shown in Fig.1. A shunt APF is connected in parallel with the load, to find its harmonic current and to inject compensating current into the system, identical with the load harmonic current. Therefore, at the point of coupling the balanced current is obtained, with the help of filters in the power system. Zero sequence (neutral) current is compensated by using the fourth-leg of 3P4W inverter.

The advantage of 4-leg inverter is to compensate neutral current by providing 4th-leg. Much less DC-link capacitance is used and has effective utilization of DC-link voltage. Fig.1. shows the power circuit of a 4-leg shunt APF connected in parallel with the 1-phase and 3-phase loads as an unbalanced and non-linear load on 3-phase 4-wire electrical distribution system. In the middle of each branch a filter inductor is connected to the power system.

One of the main objectives of the four-leg shunt APF is to procure balanced source currents by compensating unbalanced load currents. In order

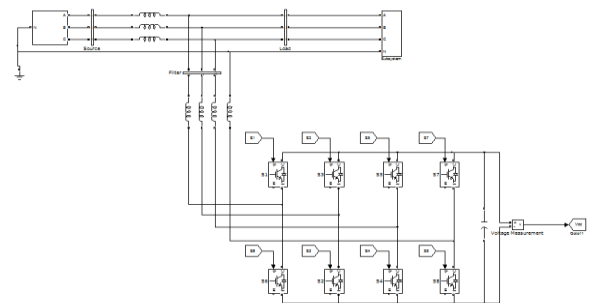


Fig-1: Four-leg VSI-based shunt APF system configuration

to generate the balanced reference source currents to control the shunt APF under distorted grid and unbalanced supply conditions, a balanced set of voltages needs to be extracted. To extract a balanced set of voltages under distorted grid voltages and unbalanced supply voltage conditions, simple balanced voltage extractor based on synchronous reference frame (SRF) theory is used.

## 2. SRF CONTROLLER

The synchronous reference frame (SRF) theory is a simple time-domain reference signal evaluation technique and it performs in steady-state or dynamic state. The supreme characteristic of SRF theory is the ease of the calculations, which includes only algebraic calculation. The SRF theory consists of direct d-q and inverse d-q park transformations as shown in Figure 2, which evaluates the specific harmonic component of the input signals [6].

### 2.1 Basic Principle

In SRF theory, stationary reference frame three-phase a-b-c system is transformed to two phase direct axis (d) and quadratic axis (q) rotating coordinate system.

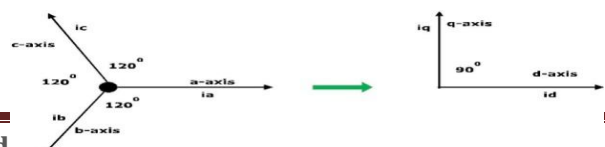


**Fig-2:** a-b-c to d-q transformation.

In a-b-c, stationary axes are isolated from each other by  $120^\circ$  and in d-q system rotating axes are isolated from each other by  $90^\circ$  as shown in Figure 2.

### 2.2 SRF Controller Implementation

Let the three distorted and unbalanced supply voltages at the point of common coupling is represented as

$$v_{sx}(t) = \sqrt{2} \sum_{n=1}^h V_{sn} \sin(n\omega t + \theta_{sn}), \quad x = a, b, c \quad (1)$$

Where subscript  $s$  denotes the supply, subscript  $x$  denotes the phase of the system,  $n$  denotes the harmonic order,  $h$  denotes the maximum harmonic order selected by the user,  $V$  denotes the rms value of the voltage,  $\theta$  denotes the phase angle. For the  $n$ -th-order harmonic the stationary three phase voltages given in equation (1) can be transformed into two axis d-q rotating reference frame using parks transformation.

$$\begin{pmatrix} v_{dn} \\ v_{qn} \end{pmatrix} = \frac{2}{3} \begin{pmatrix} \sin n(\omega t) & \cos n(\omega t) \\ \sin n(\omega t - 120) & \cos n(\omega t - 120) \\ \sin n(\omega t + 120) & \cos n(\omega t + 120) \end{pmatrix} \begin{pmatrix} v_{an}(t) \\ v_{bn}(t) \\ v_{cn}(t) \end{pmatrix} \quad (2)$$

Where,  $\omega$  is the fundamental angular frequency of the supply voltages which can be obtained by Phase Locked Loop. The d-q transformation output signals are obtained by park's transformation of unbalanced source voltages and the performance of the Phase Locked Loop (PLL). The rotation speed (rad/sec) of the rotating reference frame is provided by the PLL circuit, where  $t$  is set as fundamental frequency component.

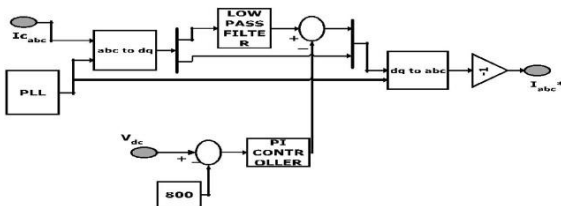


**Fig-3:** Synchronous d-q reference frame based compensation.

The  $v_{dn} - v_{qn}$  voltages are elapsed through low pass filter (LPF) which permits only the fundamental frequency components and filters out the harmonic components of the source voltages. LPF is a second order Butterworth filter, to abolish higher order harmonics cut off frequency

is to be selected. For the reference d-q signals of the DC component steady state error is eliminated using PI controller. Moreover, PI controller maintains the capacitor voltage nearly constant. DC-side capacitor voltage is sensed and compared with desired reference voltage to determine the error voltage by PWM-voltage source inverter. This error voltage is passed through a PI controller.

Using inverse Park transformation equation (3) gives the balanced set of supply voltages in the stationary reference frame for the  $n$ th harmonic.

$$\begin{pmatrix} v'_{dn}(t) \\ v'_{bn}(t) \\ v'_{cn}(t) \end{pmatrix} = \begin{pmatrix} \sin n(\omega t) & \cos n(\omega t) \\ \sin n(\omega t - 120) & \cos n(\omega t - 120) \\ \sin n(\omega t + 120) & \cos n(\omega t + 120) \end{pmatrix} \begin{pmatrix} v_{dn} \\ v_{qn} \end{pmatrix} \quad (3)$$

The above procedure is carried out for  $n = 1, 2, \dots, h$ . Therefore, the three-phase balanced set of voltages are expressed in equation (4).

$$v'_{sx}(t) = \sum_{n=1}^h v'_{sxn}(t), \quad x = a, b, c \quad (4)$$

Thus all the right-hand side quantities of equation(4) are balanced,  $v'_{sx}$  represents the balanced set of supply voltages derived from distorted grid and unbalanced supply voltages.

### 3. MAIN CONTROL APPROCH

#### 3.1 Objective Function Of Control Algorithms

There are several objectives that can be applied to the shunt APF problem which incorporate source current THD minimization, APF kilo volt ampere rating minimization, or source power factor maximization [16], [18]. The main objective considered in this algorithm is to maximize the source power factor to decrease the cost of electricity consumption under power factor-based tariff. Power factor maximization can be obtained by minimizing the square of the apparent power computed using the extracted balanced set of voltages and the required source current of any phase[19],[20].

The general Lagrangian function is formed as follows:

$$L = f + \lambda r + \mu s \quad (5)$$

where  $L$  is the Lagrangian function,  $f$  is the objective function, and  $\lambda$  and  $\mu$  are the Lagrangian multipliers. The terms  $r$  and  $s$  are the equality and inequality constrains, respectively. In the optimization process the equality constraint should supply the load average power required

for the source currents, while THD limit is specified by the inequality constraint.

### 3.2 Iterative Optimization Control Algorithm (Oca)

An optimization technique is utilized to obtain the required optimal performance between unity power factor and THD limits of source currents [17]. Iterative Optimization Control Algorithm (OCA) is appropriate only when the supply voltages are balanced and distorted. OCA results in unbalanced compensated source currents if the supply voltages are unbalanced and distorted. Therefore balanced compensated source currents can be obtained by extracting balanced set of voltages from the unbalanced distorted supply voltages.

The desired source current for phase-*a* is given in equation (6)

$$i_{sa}^*(t) = k_1(v_{sa1}^+) + k_n \left( \sum_{n=1}^k (v_{sa(2n+1)}^+) + \sum_{n=0}^k (v_{sa(2n+2)}^-(t) + v_{sa(2n+3)}^0(t)) \right) \tag{6}$$

Where  $k_1$  and  $k_n$  are conductance factors for the fundamental and the harmonics respectively. The THD content in source current can be governed by controlling conductance factors. To achieve the conductance factors for the minimum apparent power Lagrangian multiplier technique is used by fulfilling the stated constraints. For shaping the source currents the conductance factors  $k_1$  and  $k_n$  are responsible, corresponding to the constraints specified.

The conductance factors obtained for the previous load cannot be used when the load changes from one level to another. To get the new conductance factors again the optimization process has to be run for the new load. Then, the obtained new values are used in the compensation algorithm. Therefore, the iterative OCA cannot give instantaneous result.

### 3.3 Proposed Single-Step Non Iterative Optimized Algorithm

In the proposed single step control algorithm the conductance factors  $G_1, G_{H-\delta}$  and  $G_{H-\epsilon}$  are calculated directly. When compared to the iterative algorithms [19] and [20] the proposed single step control algorithm has superior performance. Under distorted grid and

unbalanced supply conditions, the following conditions should be satisfied in order to achieve the UPF operation 1) The source currents harmonic content must be same as the supply voltages harmonic contents and 2) all the phase currents must be in phase with their respective phase voltages. This shows that, in case of UPF operation, the source current THD must equate to the source voltage THD value at the same time by keeping inphase relationship with respect to the individual phase voltage. For the source current THD and UB factor exceeding the acceptable limit, the source current THD and UB factor could be maintained within the specified limits by controlling the harmonic ratios and balancing the average power equally among the three phases. To maximize the power factor and to get the aforementioned constraints of the source current, the shunt APF control algorithm is formulated by taking conductance factors  $G_n$  as main variable for each individual harmonic order in an optimization problem.

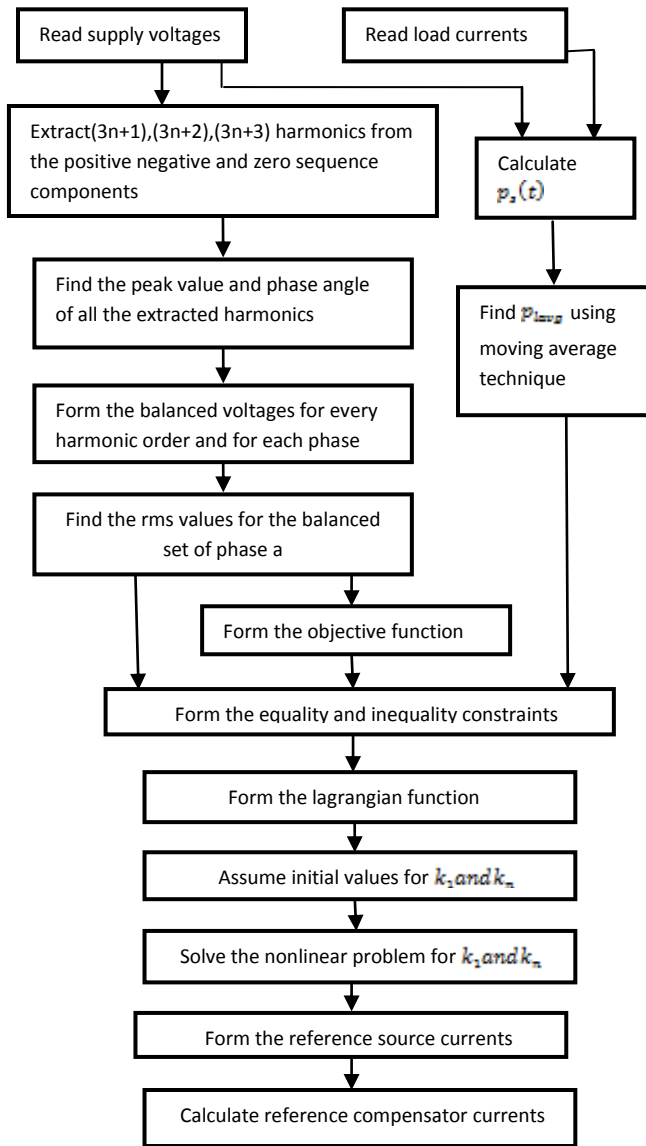


**Fig-4:** Flowchart for the extraction of reference compensator currents using iterative optimization control algorithm.

Using (4), the desired source currents can be expressed as follows.

$$i_{sx}^*(t) = G_1 v'_{sx1} + \sum_{n=2}^h G_n v'_{sxn}, \quad x = a, b, c \quad (7)$$

where  $i_{sx}^*(t)$  stands for the desired or reference quantity.  $G_1$  and  $G_n$  are the conductance factors for the fundamental and  $n$ th-order harmonic components.

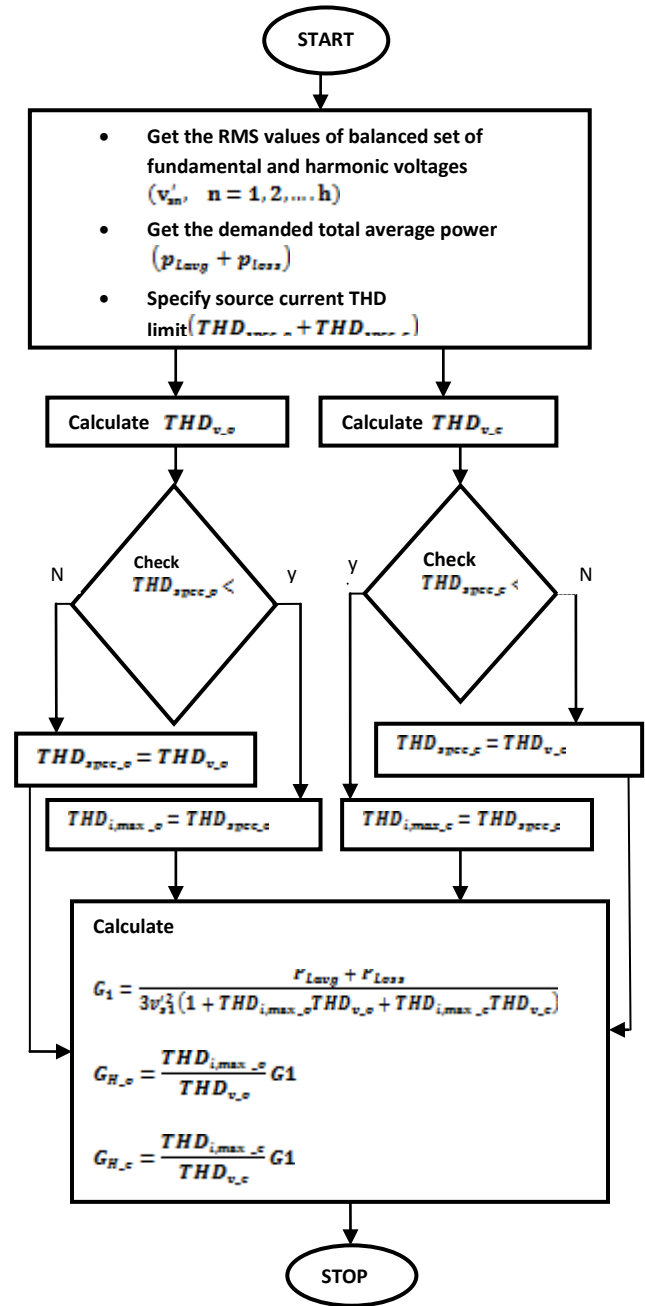


**Fig-5:** Flowchart for non iterative optimized algorithm to determine the conductance factors  $G_1, G_{H-a}$  and  $G_{H-b}$

$v'_{sx}$  represents the balanced set of supply voltages derived from the distorted grid and unbalanced supply voltages. To maximize the power factor the values of these conductance factors  $G_1$  and  $G_n$  can be controlled while satisfying the average power balance and THD constraints. The single step optimization problem can be formulated by

considering one phase, since the values of same conductance factor will be applied to other phases to achieve balanced source currents.

By using Lagrangian formulation and by applying Karush-Kuhn-Tucker optimality conditions, the following mathematical equations for the conductance factors can be derived.

$$G_1 = \frac{P_{Lavg} + P_{Loss}}{3V_{LL}^2 (1 + THD_{i,max\_o} THD_{v,o} + THD_{i,max\_e} THD_{v,e})} \quad (8)$$

$$G_{H\_o} = \frac{THD_{i,max\_o}}{THD_{v,o}} G_1 \quad (9)$$

$$G_{H\_e} = \frac{THD_{i,max\_e}}{THD_{v,e}} G_1 \quad (10)$$

Where,  $P_{Lavg}$  is the demanded average load power, which is calculated with the three-phase instantaneous source voltages and load currents.  $P_{Loss}$  is the average power, which is required to overcome the losses in the shunt APF and to maintain the dc-link capacitor voltage.  $THD_{i,max\_o}$  and  $THD_{i,max\_e}$  are the upper bounds on the source current harmonic distortion due to odd and even harmonics respectively,  $THD_{spec\_o}$  and  $THD_{spec\_e}$  are the user-defined or prespecified source current THD limits due to odd and even harmonics respectively.

The flowchart of the proposed single-step noniterative optimized algorithm to determine the conductance factors  $G_1$ ,  $G_{H\_o}$  and  $G_{H\_e}$  is shown in Fig.5. The first step in this algorithm is to get the RMS values of balanced set of fundamental and harmonic voltages.  $THD_{v,o}$  and  $THD_{v,e}$  are determined with the help of extracted balanced set of voltages.  $THD_{i,max\_o}$  and  $THD_{i,max\_e}$  will be determined by comparing  $THD_{v,o}$  and  $THD_{v,e}$  with  $THD_{spec\_o}$  and

$THD_{spec\_e}$  respectively. If  $THD_{spec\_o}$  is less than  $THD_{v,o}$ ,  $THD_{i,max\_o}$  will be set equal to  $THD_{spec\_o}$ , Otherwise the value of  $THD_{i,max\_o}$  will be set equal to  $THD_{v,o}$ . Similarly,  $THD_{i,max\_e}$  will be determined by comparing  $THD_{spec\_e}$  with  $THD_{v,e}$ . The optimal conductance factors for the fundamental, even and odd harmonics are calculated with the derived formulas (8)-(10). The flowchart is an fundamental part of the overall control block of the shunt APF.

Overall control simulink block diagram for the proposed noniterative optimized control of the four-leg VSI-based shunt APF with PI controller is shown in Fig6 and Fig.6(a). Overall control simulink block diagram is implemented for  $h=33$ . where,  $h$  is the higher harmonic order for conductance factors.

The following are the salient features of the proposed single-step optimized approach.

- 1) The iterative OCA involves 'h' conductance factors where as the proposed approach involves only three conductance factors (one for the fundamental and the other for odd and even harmonics), thus proposed approach reduces the complexity of the problem.
- 2) The dissimilar conductance factors for the odd harmonics and the even harmonics ease the selection of separate THD limits on odd and even harmonics.
- 3) The optimal conductance factors are calculated directly by using mathematical formulas (8-10) without using any iterative techniques [19], [20]. Thus the proposed algorithm is fast to respond and can reduce the computation time, when compared to previous iterative methods.
- 4) For the dynamic load variations the proposed control algorithm is more effective when compared to other iterative approaches.

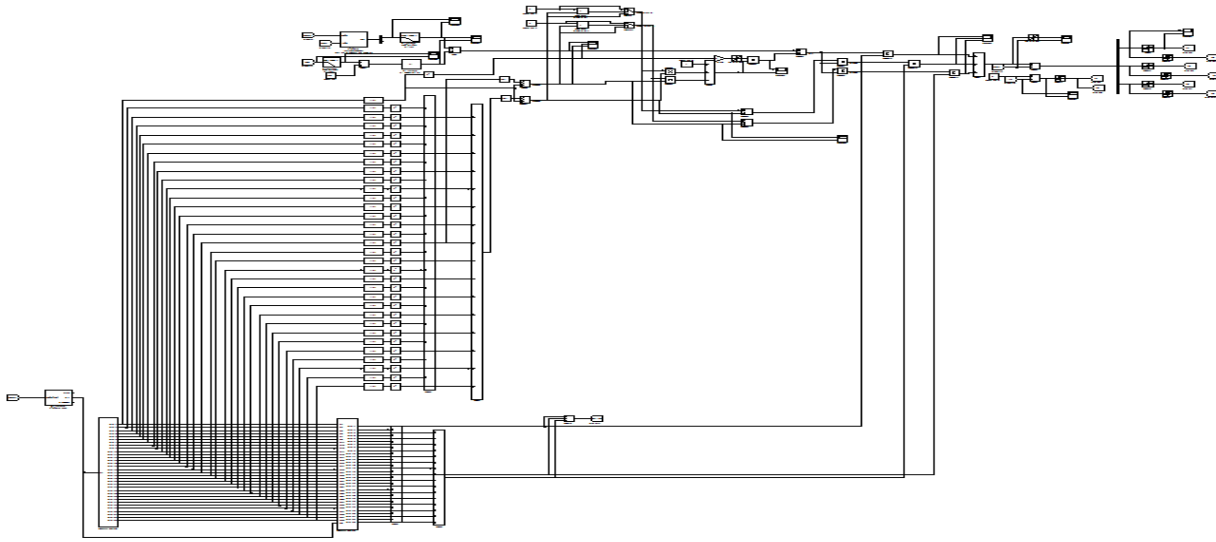


Fig-6: Overall simulink control block for the proposed noniterative optimized control of the four-leg VSI-based shunt APF.

### 3.4 OVERALL CONTROL BLOCK OF SHUNT APF

The four leg VSI based shunt APF system configuration is shown in Fig.1. The shunt APF system configuration consists of an equivalent grid behind an impedance, combined single- and three-phase loads, and the shunt APF. To realize a three phase four-wire (3P4W) APF system configuration the four-leg voltage source inverter (VSI) topology is used. To control the shunt APF under distorted grid voltages and unbalanced supply conditions, the overall control block diagram of the proposed single-step noniterative optimized control algorithm is shown in Fig.6(a).

The specified source current THD limits ( $THD_{spec_o}$  and  $THD_{spec_e}$ ), the demanded average total power ( $P_{Lavg} + P_{Loss}$ ), and the rms values of the balanced set of harmonic voltages ( $v'_{sn}$ ,  $n = 1, 2, \dots, h$ ) are the inputs to the block of single-step calculation of  $G_1, G_{H-o}$  and  $G_{H-e}$ . The demanded instantaneous load power is computed as follows.

$$P_L(t) = v_{sa}i_{La} + v_{sb}i_{Lb} + v_{sc}i_{Lc} \tag{11}$$

To obtain the average power  $P_{Lavg}$  the instantaneous power  $P_L(t)$  is then passed through an LPF. The dc-link voltage is maintained constant at a prespecified value by drawing a small amount of active power from the grid. This can be accomplished with a discrete proportional-integral (PI) controller, as in equation(12).

$$P_{L_{oss}}(k) = P_{L_{oss}}(k-1) + K_p\{e(k) - e(k-1)\} + K_i e(k) \tag{12}$$

$$\text{Where } e(k) = v_{dc}^* - v_{dc}^f(k). \tag{13}$$

Where  $v_{dc}^f(k)$  is the measured instantaneous voltage across the dc-link capacitor voltage passed through the LPF,  $v_{dc}^*$  is the reference Dc-link voltage and k is the sample number.  $k_p$  and  $k_i$  are the proportional and integral gains of the PI controller.

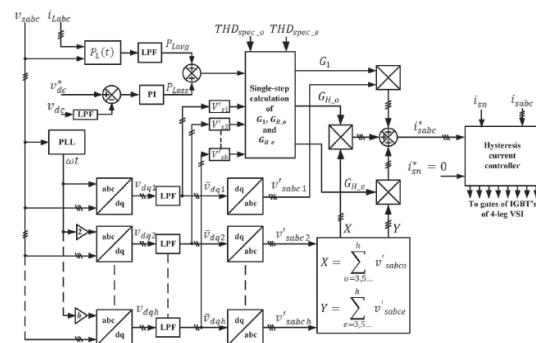


Fig-6(a): Overall control block for the proposed noniterative optimized control of the four-leg VSI-based shunt APF with PI controller.

### 4. FUZZY APPROACH

In the Fuzzy approach, the simplicity of a PI controller is succeeded with the intelligence and adaptiveness of the

fuzzy logic based control system. Therefore the Fuzzy controller is characterized as an intelligent adaptive controller. Fuzzy logic control algorithm is proposed for harmonic current and inverter dc voltage control to improve the performances of the three phase shunt active power filters. The MATLAB Fuzzy Logic Toolbox is used for implementing the fuzzy logic control algorithm. The advantage of fuzzy control is that it is based on a linguistic description and does not require a mathematical model of the system. In the presence of fuzzy controller the source current shaping is achieved with negligible amount of spikes resulting in %reduction in THD.

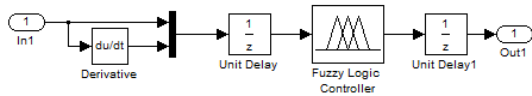


Fig-7: Fuzzy control system

Fig.7. shows the fuzzy control system. Where, In1 is the capacitor voltage error, du/dt is the change in capacitor voltage error. Rule table for the fuzzy logic controller is shown in Table1. Out1 is the output of fuzzy control system.

#### 4.1 Fuzzy Inference

The strength of the fuzzy logic system depends on fuzzy inference. The fuzzy rules of the system represent the knowledge of the system. By adjusting the weight values of the fuzzy rules, fuzzy logic system is tuned for better performance. For the proposed FC, the two input signals are capacitor voltage error and change in error are properly scaled and fuzzified. Seven membership functions are used for error, change in error and also for controller output. Linear triangular membership function is used in the design of fuzzy controller for SAF. With two input variable and each variable having seven labels there will be 49 input label pairs. A rule table relating each one of the 49 input label pairs to the respective output label is given in Table 1. The defuzzification stage produces the final crisp value. The centroid method is employed for defuzzification.

Table-1: Rule table for fuzzy logic controller.

e/de	NB	NM	NS	ZE	PS	PM	PB
NB	NB	NB	NB	NB	NM	NS	ZE
NM	NB	NB	NB	NM	NS	ZE	PS
NS	NB	NB	NM	NS	ZE	PS	PM
ZE	NB	NM	NS	ZE	PS	PM	PB

PS	NM	NS	ZE	PS	PM	PB	PB
PM	NS	ZE	PS	PM	PB	PB	PB
PB	ZE	PS	PM	PB	PB	PB	PB

The PI controller in Fig.6(a). is replaced with FUZZY controller and the results are observed. The performance of the control strategy is improved, hence THD (%) is reduced resulting in improved performance.

#### 5. ANALYSIS OF THE SIMULATION RESULTS

To verify the performance of the proposed single-step noniterative optimized control algorithm for SAPF with PI and FUZZY for both steady state and dynamic conditions are performed and compared with that of an iterative OCA algorithm, a detailed simulation study is carried out under the MATLAB/SIMULINK environment. The simulated test system data are given in Table.2 the following cases are considered.

##### A. Case 1: Unbalanced Supply Voltages Distorted With Odd Harmonics Only—Steady-State Load Condition.

The performance of the proposed optimized control algorithm is evaluated for the following three conditions: 1) HF (0% THD) operation; 2) UPF operation; and 3) a specified-THD-limit operation.

**HF (0% THD) operation:** HF mode of operation or perfect harmonic cancelation (PHC), here the objective is to compensate the fundamental reactive power demand of the load and to cancel all harmonic load current components in addition to balance the currents that are drawn from the power network. Therefore, at PCC the source current will be in phase with the fundamental positive sequence component of the voltage. The HF strategy gives sinusoidal source currents. For this case, the THD limits  $THD_{spec_o}$  and  $THD_{spec_e}$  are set equal to 0%.

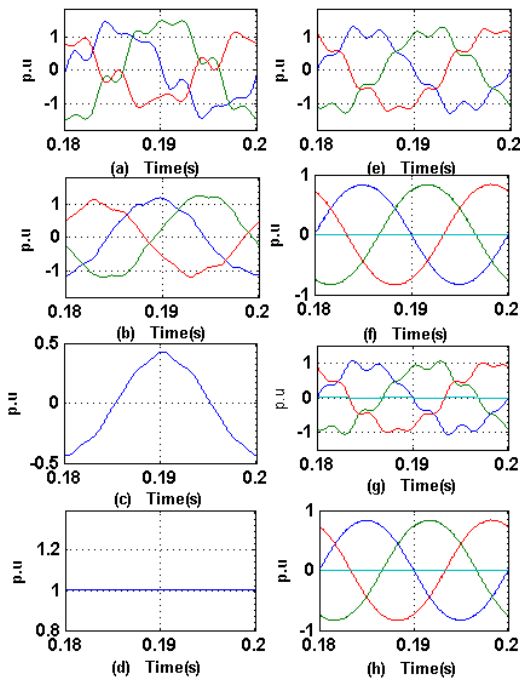


**Fig-8:** Simulation results under unbalanced supply voltages distorted with odd harmonics using the proposed single-step optimized control algorithm with FUZZY controller. (a) Supply voltages. (b) Load currents. (c) Load neutral current. (d) DC-link voltage. (e) Extracted balanced set of voltages. (f) Source currents (HF mode). (g) Source currents (UPF mode). (h) Source currents (optimized mode).[CASE1 WITH FUZZY]

The source currents after the compensation are balanced and sinusoidal and are shown in fig.8 (f). Table 3, shows the THD of the source currents with three modes of operation.

**UPF operation:** In this strategy, the load and APF are viewed by the source as a linear resistance. At the PCC source current and source voltage will have identical wave shapes with different amplitudes, after illusion of the unity power factor (UPF). For a given average load power

**Table-2:** System data for simulation

System parameters	Base voltage(AC)-415V(L-L) Base voltage(DC)-750V Base power-15KVA
Loads	L1:-3-phase diode rectifier with 20Ω resistive load L2:-phase-a:0.05+j0.15p.u Phase-b:0.05+j0.175p.u Phase-c:0.025+j0.125p.u Steady state load condition:L1+L2 Dynamic load condition: load is changed from L1 to L1+L2 and again brought back to L1
APF	DC link capacitor-2000μF; Reference DC link voltage=750v; inductor=6mH

**Table -3:** Source current

THD (%) [case1]

Mode	Strategy	THD (%)		
		a	B	C
HF	Proposed with fuzzy	0.88	0.75	0.81
	Proposed with PI	1.68	1.72	1.77
	OCA	1.78	1.8	1.86
UPF	Proposed with fuzzy	7.29	7.65	7.51
	Proposed with PI	14.43	14.53	5.65
	OCA	14.43	14.53	14.62
Opti-mized	Proposed with fuzzy	2.78	2.81	2.82
	Proposed with PI	5.55	5.63	5.65
	OCA	5.48	5.6	5.6

implementation of a UPF control strategy gives minimum RMS values of source current. source currents have to be of same shape, harmonics, unbalance, and in phase with the respective phase voltages.

Similarly, in PHC strategy the compensated source currents will not allow any harmonic component. Utmost existing works on shunt active power filters under distorted and unbalanced supply voltages admits either one of the two control strategies (PHC or UPF). In order to utilize the advantages of both the strategies, there should be an optimal operation between these two important compensation characteristics.

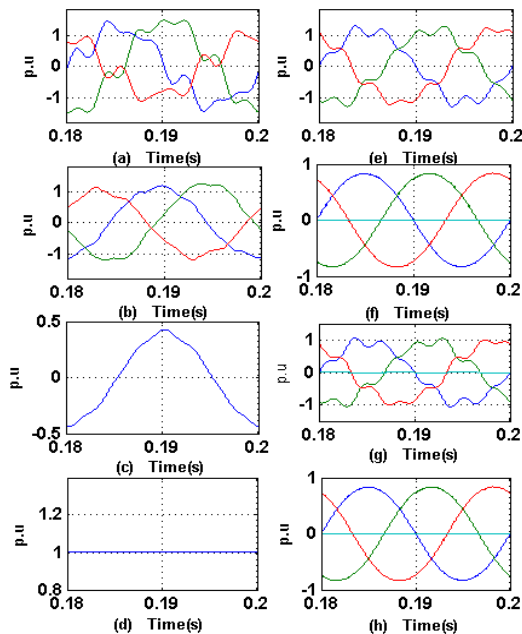


**Fig-9:** Simulation results under unbalanced supply voltages distorted with odd harmonics using the proposed single-step optimized control algorithm with PI controller. (a) Supply voltages. (b) Load currents. (c) Load neutral current. (d) DC-link voltage. (e) Extracted balanced set of voltages. (f) Source currents (HF mode). (g) Source currents (UPF mode). (h) Source currents (optimized mode).[CASE1 WITH PI]

In UPF operation, to test the controller performance, the odd and even THD limits were specified as 100%. As shown in the flowchart Fig.5, the proposed algorithm compares the specified THD limits  $THD_{spec_o}$  and  $THD_{spec_e}$  of 100% with the balanced set of source voltage THDs. The specified THD limits of 100% are greater than the balanced set of supply voltage THDs, and therefore, the

control algorithm operates in the UPF mode to achieve the maximum possible power factor operation. Fig.9(g) illustrates the compensated source currents when the APF system operates in the UPF operation. Finally, the performance of the proposed single-step optimized control algorithm is evaluated considering constraints on source current THD levels while maximizing the power factor.

In optimized mode of operation the THD limits of the source currents are specified as 5%. Fig. 9(h) depicts the simulation results under the optimized mode of operation. From the previously discussed three modes that the compensated source current profile in the optimized mode is in between HF and UPF operations. In all the aforementioned operating modes, the fourth leg of the shunt APF effectively compensates the load neutral current [Fig. 9(c)] and thus reduces the source-side neutral current to zero.

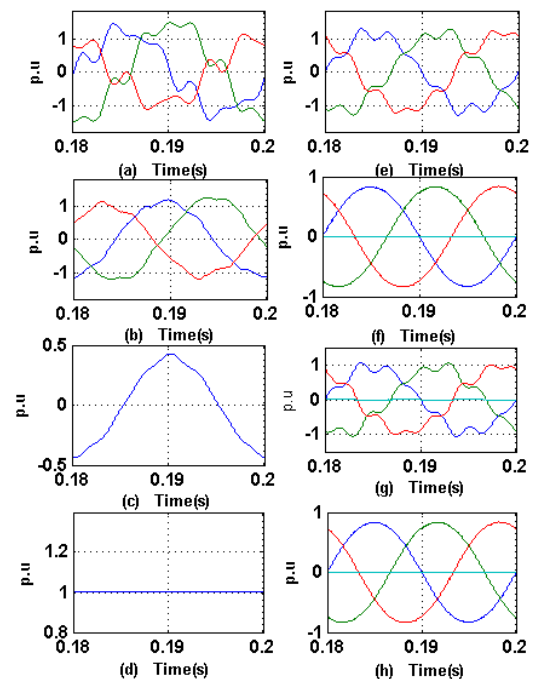


**Fig-10:** Simulation results under unbalanced supply voltages distorted with odd harmonics using OCA. (a) Supply voltages. (b) Load currents. (c) Load neutral current. (d) DC-link voltage. (e) Extracted balanced set of voltages. (f) Source currents (HF mode). (g) Source currents (UPF mode). (h) Source currents (optimized mode).[CASE1 WITH OCA]

The simulated results are shown in fig.8 and fig.9 for the proposed single-step optimized algorithm with PI and Fuzzy controllers for the system under three operating

modes (HF, UPF, and optimized). When PI controller is replaced with Fuzzy controller, in Fig.6(a) the performance of the proposed single-step optimized algorithm with fuzzy is observed, source current THD can be reduced with Fuzzy. The THD value of source currents obtained with PI, Fuzzy controller and OCA is shown in the Table.3

The simulated results for the iterative OCA algorithm are shown in Fig.10, under three operating modes (HF, UPF, and optimized). The proposed non iterative optimized method, however, requires minimum computational burden compared to the OCA method without any iterative technique. Since the model relies on only three control variables  $G_L$ ,  $G_{H-o}$  and  $G_{H-s}$  and the direct computation of the variables.. Table.3 gives the comparison between iterative OCA and the proposed single step optimized control method for SAPF with PI and Fuzzy controller.

**B. Case 2: Unbalanced Supply Voltages Distorted With Odd Harmonics Only—Dynamic Load Condition.**

The proposed control algorithm distorted with odd harmonics during a sudden load change condition is illustrated in Fig. 11 and Fig.12. To create the dynamic condition, at time t=0.2s the load is changed from L1 to L1+L2 (Table.2) and again brought back to L1 at time t=0.3s. The change in the load current profile can be viewed from Fig. 11.(b). The compensated source current profile is shown in Fig. 11.(c). As noticed, the APF system with the proposed single-step optimized approach achieves the new steady-state condition within one cycle and without affecting the APF compensation capability during both load increase and decrease. Furthermore, the dc-link controller, as shown in Fig.11.(d), effectively regulates the dc-bus voltage at the set reference value.

The simulated results are shown in fig.11 and fig.12 for the proposed single-step optimized algorithm with PI and fuzzy controllers for the system under optimized mode for dynamic load condition under unbalanced supply voltages distorted with odd harmonics. The PI controller in Fig.6(a) is replaced with Fuzzy controller and the performance of the proposed single-step optimized algorithm with fuzzy controller is observed.

Under the same dynamic condition, the performance of the iterative OCA method is shown in Fig.13. As observed from Fig. 13(a), the compensated source currents are not balanced. In addition, the dc-link voltage, shown in Fig.13(b) settles at a new operating point, lower than the set reference value. This is mainly due to computational delay in calculating the new conductance factors. Therefore, the iterative OCA-based controller tries to

compensate the source currents based on the previously computed conductance factors, and thus, the source current become more distorted and unbalanced.

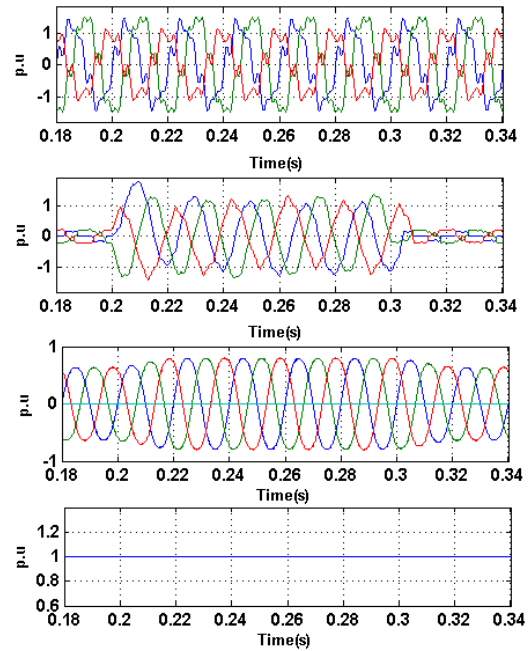


**Fig-11:** Simulation results for dynamic load condition under unbalanced supply voltages distorted with odd harmonics using the proposed algorithm With PI (a) Supply voltages. (b) Load currents. (c) Source currents (optimized mode). (d) DC-link voltage.[CASE2 WITH PI]

**Table-4:** Source currents THD(%) for dynamic mode of operation.

Method		Propose d with FUZZY	Propose d with PI	OCA
THD (%)	a	2.78	5.53	5.45
	b	2.81	5.63	5.61
	c	2.82	5.66	5.61

Therefore, Table 4 presents the compensated source current THDs for SAPF with PI, Fuzzy and OCA. Thus, this dynamic condition demonstrates the true capability and enhanced performance of the proposed single-step optimized algorithm over other iterative optimization-based approaches.

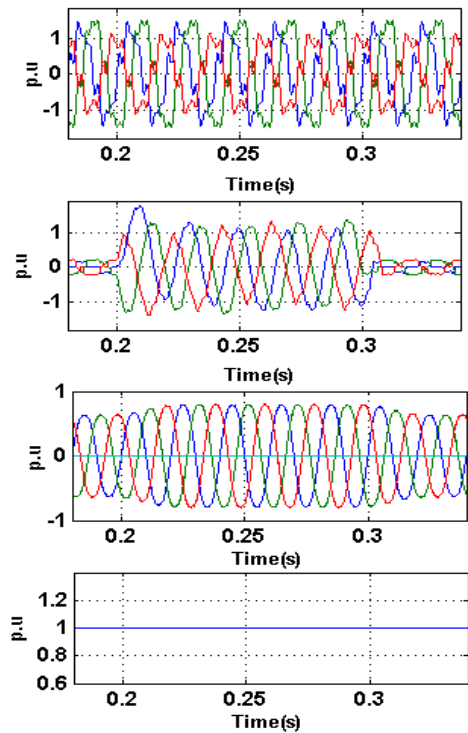


**FIG-12:** Simulation results for dynamic load condition under unbalanced supply voltages distorted with odd harmonics using the proposed algorithm with FUZZY (a) Supply voltages. (b) Load currents. (c) Source currents (optimized mode). (d) DC-link voltage. [CASE2 WITH FUZZY]

**Table-5:** Distorted and unbalanced supply voltages (case1 and case2).

Phase a	Phase b	Phase c
$Sin(wt-10)$ $+0.2sin(5(wt+6))$ $+0.14sin(7(wt-6))$	$1.2sin(wt-100)$ $+0.16sin(5(wt-124))$ $+0.17sin(7(wt-116))$	$0.8sin(wt+100)$ $+0.24sin(5(wt+124))$ $+0.11sin(7(wt+116))$

**C. Case 3: Unbalanced Supply Voltages Distorted With Both Odd and Even Harmonics—Steady-State Load Condition.**

The simulated results are shown in Fig.14 and Fig.15 for the proposed single-step optimized algorithm with Fuzzy and PI controllers for the system under optimized mode

for steady state load condition under unbalanced supply voltages distorted with both odd and even harmonics.

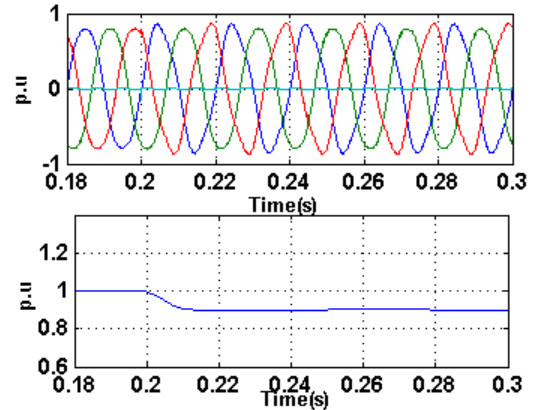


**Fig-13:** Simulation results for dynamic load condition under unbalanced supply voltages distorted with odd harmonics using an iterative optimization method. (a) Source currents (optimized mode). (b) DC-link voltage.[CASE2 WITH OCA]

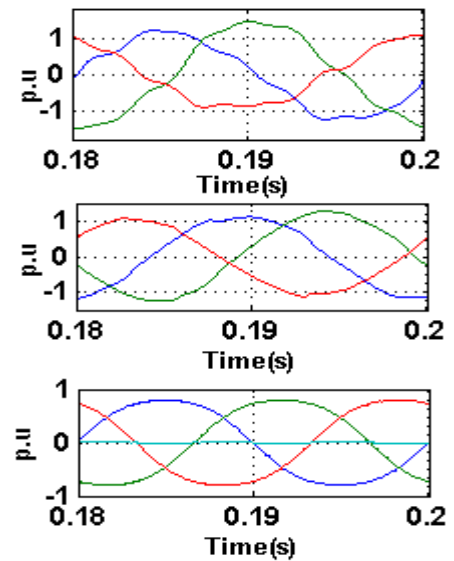


**Fig-14.** Simulation results under unbalanced supply voltages distorted with both odd and even harmonics using the proposed optimized control algorithm with FUZZY. (a) Supply voltages. (b) Load currents. (c) Source currents.[CASE3 WITH FUZZY]

The profiles of the supply voltages and load currents with Fuzzy controller are shown in Fig.14(a) and 14(b). The source currents for SAPF with Fuzzy controller are shown

in Fig.14(c). The superiority of the proposed algorithm with PI and Fuzzy, over OCA in terms of computation time was highlighted in the previous two cases (case1 and case2). In order to show the advantage of having different THD limits on odd and even harmonics, the performance of the proposed algorithm is evaluated and compared with that of OCA under unbalanced supply voltages distorted with both even and odd harmonics (Table.6). The profiles of the supply voltages and load currents are given in Fig. 15(a) and (b). The compensated source currents using the proposed algorithm are shown in Fig. 15(c), while Fig. 15(d) depicts the source currents using OCA.

**Table-6:** Distorted and unbalanced supply voltages (case3).

Phase a	Phase b	Phase c
$\sin(wt-10)$	$1.2\sin(wt-100)$	$0.8\sin(wt+100)$
$+0.06\sin(2(wt+5))$	$+0.04\sin(2(wt-128))$	$+0.06\sin(2(wt-128))$
$+0.05\sin(4(wt+6))$	$+0.04\sin(4(wt-124))$	$+0.06\sin(4(wt+124))$
$+0.05\sin(5(wt+6))$	$+0.04\sin(5(wt-124))$	$+0.06\sin(5(wt+124))$
$+0.05\sin(7(wt-6))$	$+0.06\sin(7(wt-116))$	$+0.04\sin(7(wt+116))$

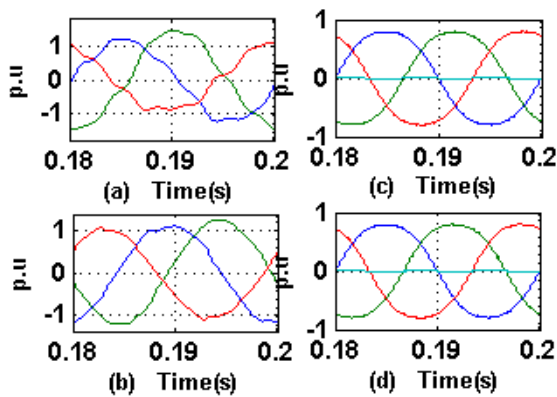


**Fig-15.** Simulation results under unbalanced supply voltages distorted with both odd and even harmonics using the proposed optimized control algorithm with PI and OCA. (a) Supply voltages. (b) Load currents. (c) Source currents (proposed algorithm with PI). (d) Source currents (OCA).[CASE3 WITH PI AND OCA]

## 6. CONCLUSIONS

To achieve an optimum performance between power factor and THD a new control approach for a three-phase four-wire shunt active power filter with PI and Fuzzy controller under distorted grid voltage and unbalanced supply conditions has been proposed. To see the electrical phenomenon factors the planned optimized approach is

simple and straight forward to implement. Hence, it doesn't need iterative optimization techniques.

It's presented mathematically that solely three electrical phenomenon factors (one for the basic harmonic and two alternative for odd and even harmonics) measure decent to see the required reference supply currents. The planned algorithmic program determines the electrical phenomenon factors in ten  $\mu s$ , hence planned optimized approach is appropriate under dynamically changing load conditions (other iterative optimization-based approaches are confined to steady-state conditions). Thus source current THD (%) is reduced with Fuzzy control approach.

## REFERENCES

- [1] W. Mack Grady and S. Santoso, "Understanding power system harmonics," IEEE Power Eng. Rev., vol. 21, no. 11, pp. 8–11, Nov. 2001.
- [2] B. Singh, K. Al-Haddad, and A. Chandra, "A review of active filters for power quality improvement," IEEE Trans. Ind. Electron., vol. 46, no. 5, pp. 960–971, Oct. 1999.
- [3] Y. Tang, P. C. Loh, P. Wang, F. H. Choo, F. Gao, and F. Blaabjerg, "Generalized design of high performance shunt active power filter with output LCL filter," IEEE Trans. Ind. Electron., vol. 59, no. 3, pp. 1443–1452, Mar. 2012.
- [4] M. Angulo, J. Lago, D. Ruiz-Caballero, S. Mussa, and M. Heldwein, "Active power filter control strategy with implicit closed loop current control and resonant controller," IEEE Trans. Ind. Electron., vol. 6, no. 7, pp. 2721–2730, Jul. 2013.
- [5] A. Bhattacharya and C. Chakraborty, "A shunt active power filter with enhanced performance using ANN-based predictive and adaptive controllers," IEEE Trans. Ind. Electron., vol. 58, no. 2, pp. 421–428, Feb. 2011.
- [6] G. W. Chang and T.-C. Shee, "A novel reference compensation current strategy for shunt active power filter control," IEEE Trans. Power Del., vol. 19, no. 4, pp. 1751–1758, Oct. 2004.
- [7] T. E. Nunez-Zuniga and J. A. Pomilio, "Shunt active power filter synthesizing resistive loads," IEEE Trans. Power Electron., vol. 17, no. 2, pp. 273–278, Mar. 2002.
- [8] S. K. Jain, P. Agarwal, and H. O. Gupta, "A control algorithm for compensation of customer-generated harmonics and reactive power," IEEE Trans. Power Del., vol. 19, no. 1, pp. 357–366, Jan. 2004.

- [9] S.-J. Huang and J.-C. Wu, "A control algorithm for three-phase three-wired active power filters under nonideal mains voltages," *IEEE Trans. Power Electron.*, vol. 14, no. 4, pp. 753–760, Jul. 1999.
- [10] C.-C. Chen and Y.-Y. Hsu, "A novel approach to the design of a shunt active filter for an unbalanced three-phase four-wire system under nonsinusoidal conditions," *IEEE Trans. Power Del.*, vol. 15, no. 4, pp. 1258–1264, Oct. 2000.
- [11] A. Chandra, B. Singh, B. N. Singh, and K. Al-Haddad, "An improved control algorithm of shunt active filter for voltage regulation, harmonic elimination, power-factor correction, and balancing of nonlinear loads," *IEEE Trans. Power Electron.*, vol. 15, no. 3, pp. 495–507, May 2000.
- [12] V. M. Moreno, A. P. Lopez, and R. I. D. Garcias, "Reference current estimation under distorted line voltage for control of shunt active power filters," *IEEE Trans. Power Electron.*, vol. 19, no. 4, pp. 988–994, Jul. 2004.
- [13] M. I. M. Montero, E. R. Cadaval, and F. B. Gonzalez, "Comparison of control strategies for shunt active power filters in three-phase four-wire systems," *IEEE Trans. Power Electron.*, vol. 22, no. 1, pp. 229–236, Jan. 2007.
- [14] A. E. Emanuel, "Powers in nonsinusoidal situations—A review of definitions and physical meaning," *IEEE Trans. Power Del.*, vol. 5, no. 3, pp. 1377–1389, Jul. 1990.
- [15] S. M.-R. Rafiei, H. A. Toliyat, R. Ghazi, and T. Gopalarathnam, "An optimal and flexible control strategy for active filtering and power factor correction under non-sinusoidal line voltages," *IEEE Trans. Power Del.*, vol. 16, no. 2, pp. 297–305, Apr. 2001.
- [16] G. W. Chang and C. M. Yeh, "Optimisation-based strategy for shunt active power filter control under non-ideal supply voltages," *Proc. Inst. Elect. Eng.—Elect. Power Appl.*, vol. 152, no. 2, pp. 182–190, Mar. 4, 2005.
- [17] G. W. Chang, C.-M. Yeh, and W.-C. Chen, "Meeting IEEE-519 current harmonics and power factor constraints with a three-phase three-wire active power filter under distorted source voltages," *IEEE Trans. Power Del.*, vol. 21, no. 3, pp. 1648–1654, Jul. 2006.
- [18] G. W. Chang, "A new approach for optimal shunt active power filter control considering alternative performance indices," *IEEE Trans. Power Del.*, vol. 21, no. 1, pp. 406–413, Jan. 2006.
- [19] S. George and V. Agarwal, "A DSP based optimal algorithm for shunt active filter under nonsinusoidal supply and unbalanced load conditions," *IEEE Trans. Power Electron.*, vol. 22, no. 2, pp. 593–601, Mar. 2007.
- [20] K. R. Uyyuru, M. K. Mishra, and A. Ghosh, "An optimization-based algorithm for shunt active filter under distorted supply voltages," *IEEE Trans. Power Electron.*, vol. 24, no. 5, pp. 1223–1232, May 2009.